

Finite Temperature Field Theory and Phase Transitions

M.-P. Lombardo *

Istituto Nazionale di Fisica Nucleare, Sezione di Padova e Gruppo Collegato di Trento, Italy

*Lectures given at the:
Summer School on Astroparticle Physics and Cosmology
Trieste, 12–30 June 2000*

LNS

*lombardo@science.unitn.it

Abstract

These lectures review phases and phase transitions of the Standard Model, with emphasis on those aspects which are amenable to a first principle study. Model calculations and theoretical ideas of practical applicability are discussed as well. Contents: 1. Overview; 2. Field Theory at Finite Temperature and Density; 3. Critical Phenomena; 4. Electroweak Interactions at Finite Temperature; 5. Thermodynamics of Four Fermions models; 6. The Phases of QCD; 7. QCD at Finite Temperature, $\mu_B = 0$; 8. QCD at Finite Temperature, $\mu_B \neq 0$.

Contents

1	Overview	1
2	Equilibrium Field Theory at Finite Temperature	2
2.1	Functional Integral Representation of \mathcal{Z}	2
2.2	The Idea of Dimensional Reduction	4
2.3	Mode Expansion and Decoupling	5
2.4	Finite Temperature–Summary	5
3	Critical Phenomena	6
3.1	The Equation of State and the Critical Exponents	6
3.2	The Effective Potential	8
3.3	A Case Study	9
3.4	Dynamical Symmetry Breaking	10
4	Electroweak Interactions at Finite Temperature	11
4.1	Perturbative Analysis	11
4.2	Four Dimensional Lattice Study	13
4.3	Three Dimensional Effective Analysis	14
4.4	The Phase Diagram of the EW Sector of the Standard Model	14
5	Thermodynamics of Four Fermions Models	15
6	The Phases of QCD	19
7	QCD at Finite Temperature, $\mu_B = 0$	20
7.1	QCD High T P.T., and Symmetries I : $m_q = 0$ and the Chiral Transition	22
7.2	Two Color QCD I	23
7.3	QCD High T p.t., and Symmetries II : $m_q = \infty$ and the Confinement Transition	23
7.4	Two Color QCD II	24
7.5	Summary and Open Questions for the QCD High T Transition	25
8	QCD at Finite Temperature, $\mu_B \neq 0$	26
8.1	The Lattice Strong Coupling Analysis of the QCD Phase Diagram	27
8.2	The Phase Diagram of Two Color QCD	28
8.3	The Phase Diagram of QCD	30
	References	32

1 Overview

The aim of these lectures is mostly practical: I would like to describe the status of our understanding of phases, and phase transitions of the Standard Model relevant to cosmology and astrophysics, and to provide the tools to follow the current literature. My goal is to present results obtained from first principle calculations, together with open problems. Theoretical ideas which have inspired model builders, and the results coming from such model calculations will be discussed as well.

The main phenomena are the ElectroWeak finite temperature transition, occurring at an energy $O(100 \text{ GeV})$ and the QCD finite temperature transition(s), occurring at energies $O(100 \text{ MeV})$, within the range of current experiments at CERN and Brookhaven. The role of a (small) baryon density in QCD will be considered as well.

Only the equilibrium theory shall be considered. The main reasons are, firstly that equilibrium statistical mechanics is enough to characterize many aspects of these phase transitions, secondly that, at variance with non-equilibrium, equilibrium techniques are well consolidated, and at least some interesting results are already on firm ground. The last but not the least element in this choice is, of course, my personal expertise.

The material is organised as follows: Section 2 reviews a few basic ideas, including the general idea of dimensional reduction, and universality. Section 3 collects those basic facts on phase transitions, critical phenomena, and spontaneous symmetry breaking which are relevant to the rest. Section 4 discusses the high temperature Electroweak transition: there, the perturbative version of dimensional reduction will be seen at work, and the role of lattice studies in elucidating crucial aspects of the Standard Model will be emphasized. Section 5 introduces fermions, offers the opportunity of contrasting lattice and $1/N$ expansion results, and presents the phase diagram of four fermion models, which have a similar chiral symmetry as QCD. A general discussion on the phases of QCD, and qualitative aspects of phase transitions, is given in Section 6. Section 7 presents the status of the high temperature QCD studies, discusses in detail the symmetry aspects of confinement and chiral transition, and the “non-perturbative” dimensional reduction. In Section 8 we study QCD with a non-zero baryon density. The results for the phase diagram of the two color model are discussed in detail, together with the problems and possibility for an ab initio study of three color QCD. In addition, it is stressed that lattice not only makes a numerical “exact” study possible, but it is also amenable to an analytic treatment: the strong coupling expansion. We conclude by reviewing recent work which, combining universality arguments, model calculations and lattice results, suggests the existence of a genuine critical point in the QCD phase diagram.

Recent reviews and further readings include [1] [2] [3] [4] [5]. Closely related aspects not covered here include non-equilibrium phenomena [6], recent developments on the high temperature expansion in QCD [12], beyond-the-standard-model developments [7], [8], model calculations in the high density phase of QCD [13].

2 Equilibrium Field Theory at Finite Temperature

The basic property of equilibrium field theory is that one single function, \mathcal{Z} , the grand canonical partition function, determines completely the thermodynamic state of a system

$$\mathcal{Z} = \mathcal{Z}(\mathcal{V}, T, \mu) \quad (1)$$

\mathcal{Z} is the trace of the density matrix of the system $\hat{\rho}$

$$\mathcal{Z} = \text{Tr} \hat{\rho} \quad (2)$$

$$\hat{\rho} = e^{-(H - \mu \hat{N})/T} \quad (3)$$

H is the Hamiltonian, T is the temperature and \hat{N} is any conserved number operator. In practice, we will only concern ourselves with the fermion (baryon) number.

Remember that \mathcal{Z} determines the system's state according to:

$$P = T \frac{\partial \ln \mathcal{Z}}{\partial V} \quad (4)$$

$$N = T \frac{\partial \ln \mathcal{Z}}{\partial \mu} \quad (5)$$

$$S = \frac{\partial T \ln \mathcal{Z}}{\partial T} \quad (6)$$

$$E = -PV + TS + \mu N \quad (7)$$

while physical observables $\langle O \rangle$ can be computed as

$$\langle O \rangle = \text{Tr} O \hat{\rho} / \mathcal{Z} \quad (8)$$

Any of the excellent books on statistical field theory and thermodynamics can provide a more detailed discussion of these points. I would like to underscore, very shortly, that the problem is to learn how to represent \mathcal{Z} at non zero temperature and baryon density, and to design a calculational scheme. In this introductory chapter we will be dealing with the first of these tasks. Interestingly, the representation of \mathcal{Z} which we review in the following naturally leads to an important theoretical suggestion, namely dimensional reduction.

2.1 Functional Integral Representation of \mathcal{Z}

Consider the transition amplitude for returning to the original state ϕ_a after a time t

$$\langle \phi_a | e^{-iHt} | \phi_a \rangle = \int d\pi \int_{\phi(x,0)=\phi_a(x)}^{\phi(x,t)=\phi_a(x)} d\phi e^{i \int_0^t dt \int d^3x (\pi(\vec{x},t) \frac{\partial \phi(\vec{x},t)}{\partial t} - H(\pi, \phi))} \quad (9)$$

Compare now the above with expression (2) for \mathcal{Z} , and make the trace explicit:

$$\mathcal{Z} = \text{Tr} e^{-\beta(H - \mu \hat{N})} = \int d\phi_a \langle \phi_a | e^{-\beta(H - \mu N)} | \phi_a \rangle \quad (10)$$

We are naturally lead to the identification

$$\beta \equiv \frac{1}{T} \rightarrow it \quad (11)$$

In Figure 1 we give a sketchy view of a field theory on an Euclidean space. Ideally, the space directions are infinite, while the reciprocal of the (imaginary) time extent gives the physical temperature. We note that studying nonzero temperature on a lattice [16] is straightforward: one just takes advantage of the finite temporal extent of the lattice, while keeping the space directions much larger than any physical scale in the system.

Imaginary time

and

Inverse
Temperature

d-dimensional space

Figure 1: Sketchy view of the d+1 dimensional Euclidean space. The imaginary time is the inverse of the physical temperature of the system.

We need now to specify the boundary conditions for the fields. Let us introduce the integral $S(\phi, \psi)$ of the Lagrangian density (from now on we will always use $1/T$ as the upper extremum for the time integration).

$$S(\phi, \psi) = \int_0^{1/T} dt \int d^d x \mathcal{L}(\phi, \psi) \quad (12)$$

\mathcal{Z} is now written as

$$\mathcal{Z} = \int d\phi d\psi e^{-S(\phi, \psi)} \quad (13)$$

To find out the boundary condition for the fields, we study the thermal Green functions describing propagation from point $(\vec{y}, t = 0)$ to point $(\vec{x}, t = \tau)$ Consider the bosons first:

$$G_B(\vec{x}, \vec{y}; \tau, 0) = Tr\{\hat{\rho} T_\tau[\hat{\phi}(\vec{x}, \tau)\hat{\phi}(\vec{y}, 0)]\}/\mathcal{Z} \quad (14)$$

where T_τ is the imaginary time ordering operator:

$$T_\tau[\hat{\phi}(\tau_1)\hat{\phi}(\tau_2)] = \hat{\phi}(\tau_1)\hat{\phi}(\tau_2)\theta(\tau_1 - \tau_2) + \hat{\phi}(\tau_2)\hat{\phi}(\tau_1)\theta(\tau_2 - \tau_1) \quad (15)$$

Use now the commuting properties of the imaginary time ordering evolution and H:

$$[T_\tau, e^{-\beta H}] = 0 \quad (16)$$

togheter with the Heisenberg time evolution

$$e^{\beta H} \phi(\vec{y}, 0) e^{-\beta H} = \phi(\vec{y}, \beta) \quad (17)$$

to get:

$$G_B(\vec{x}, \vec{y}; \tau, 0) = G_B(\vec{x}, \vec{y}; \tau, \beta) \quad (18)$$

which implies

$$\hat{\phi}(\vec{x}, 0) = \hat{\phi}(\vec{x}, \beta) \quad (19)$$

Now the fermions. Everything proceeds exactly in the same way, but for a crucial difference: a minus sign in the imaginary time ordering coming from Fermi statistics:

$$T_\tau[\hat{\psi}(\tau_1)\hat{\psi}(\tau_2)] = \hat{\psi}(\tau_1)\hat{\psi}(\tau_2)\theta(\tau_1 - \tau_2) - \hat{\psi}(\tau_2)\hat{\psi}(\tau_1)\theta(\tau_2 - \tau_1) \quad (20)$$

yielding:

$$\hat{\psi}(\vec{x}, 0) = -\hat{\psi}(\vec{x}, \beta) \quad (21)$$

Hence, fermions obey antiperiodic boundary conditions in the time direction.

2.2 The Idea of Dimensional Reduction

Consider again Figure 1: it is intuitive that when the smallest significant length scale of the system $l \gg 1/T$ the system becomes effectively d-dimensional. This observation opens the road to the possibility of a simple description of many physical situations (see for instance [17] for a recent review). It is also often combined with the observation that the description of the system can be effectively ‘coarse grained’, ignoring anything which happens on a scale smaller than l . Again, this can be pictured in an immediate way on a discrete lattice: the original system can be firstly discretized on the Euclidean d+1 dimensional space, then dimensionally reduced to a d dimensional space, and finally coarse grained, still in d dimensions.

In Figure 2.2 we give a cartoon for this two steps procedure: It should be clear that,

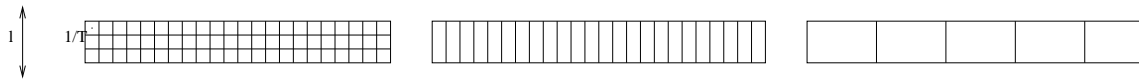


Figure 2: Sketchy view of the dimensional reduction from d+1 to d dimensions (from the leftmost to the middle picture) and subsequent coarse graining (from middle to rightmost)

despite the simplicity and elegance of the idea, both steps are far from trivial. In Section 4 we will discuss the application of these ideas to the Electroweak interactions at high temperature, where the dimensional reduction will be carried out with the help of perturbation theory. In Section 7 we will discuss dimensional reduction and universality for the QCD high temperature transitions, where the procedure relies on the analysis of system’s symmetries.

In general, there are two typical situations in which these ideas can be tried:

1. The temperature is much higher than any mass. This is the basis for the high temperature dimensional reduction, like, for instance, in the high T electroweak interactions.
2. The system is approaching a continuous transition: the correlation length of the system ξ is diverging. In such a situation all the physics is dominated by long wavelength modes. Not only the system gets effectively reduced, but the coarse graining procedure becomes doable. As an effect of this procedure, systems which are very different from one another might well be described by the same model, provided that the long range physics is regulated by the same global symmetries: this is the idea of universality which provides the theoretical framework for the study of the high T QCD transition [20].

2.3 Mode Expansion and Decoupling

Fermions and bosons behave differently at finite temperature. Consider infact the mode expansion for bosons:

$$\phi(x, t) = \sum_{\omega_n=2n\pi T} e^{i\omega_n t} \phi_n(x) \quad (22)$$

where the periodic boundary conditions for the bosons have been taken into account, and the analogous for fermions, when boundary conditions become antiperiodic:

$$\psi(x, t) = \sum_{\omega_n=(2n+1)\pi T} e^{i\omega_n t} \psi_n(x) \quad (23)$$

In the expression for the Action

$$S(\phi, \psi) = \int_0^{1/T} dt \int d^d x \mathcal{L}(\phi, \psi) \quad (24)$$

the integral over time can then be traded with a sum over modes, and we reach the conclusion that a d+1 statistical field theory at $T > 0$ is equivalent to a d-dimensional theory with an infinite number of fields.

Dimensional reduction means that only one relevant field survives: this is only possible for the zero mode of bosons.

2.4 Finite Temperature—Summary

- The partition function \mathcal{Z} has the intepretation of the partition function of a statistical field theory in d+1 dimension, where the temperature has to be identified with the reciprocal of the (imaginary) time.
- The fields' boundary conditions follows from the Bose and Fermi statistics

$$\phi(t = 0, \vec{x}) = \phi(t = 1/T, \vec{x}) \quad (25)$$

$$\psi(t = 0, \vec{x}) = -\psi(t = 1/T, \vec{x}) \quad (26)$$

i.e. fermionic and bosonic fields obey antiperiodic and periodic boundary conditions in time.

- “Dimensional reduction”, when ‘true’ means that the system become effectvely 3-dimensional. In this case only the Fourier component of each Bose field with vanishing Matsubara frequency will contribute to the dynamics, while Fermions would decouple.
- The scenario above is very plausible and physically well founded, but it is by no means a theorem. Ab initio calculations can confirm or disprove it.

We conclude this Section by coming back to the first equation, the one defining the partition funcion \mathcal{Z} . All we did so far is to write down \mathcal{Z} for a finite temperature and density in the imaginary time formalism, and to examine some immediate consequences of such a representation.

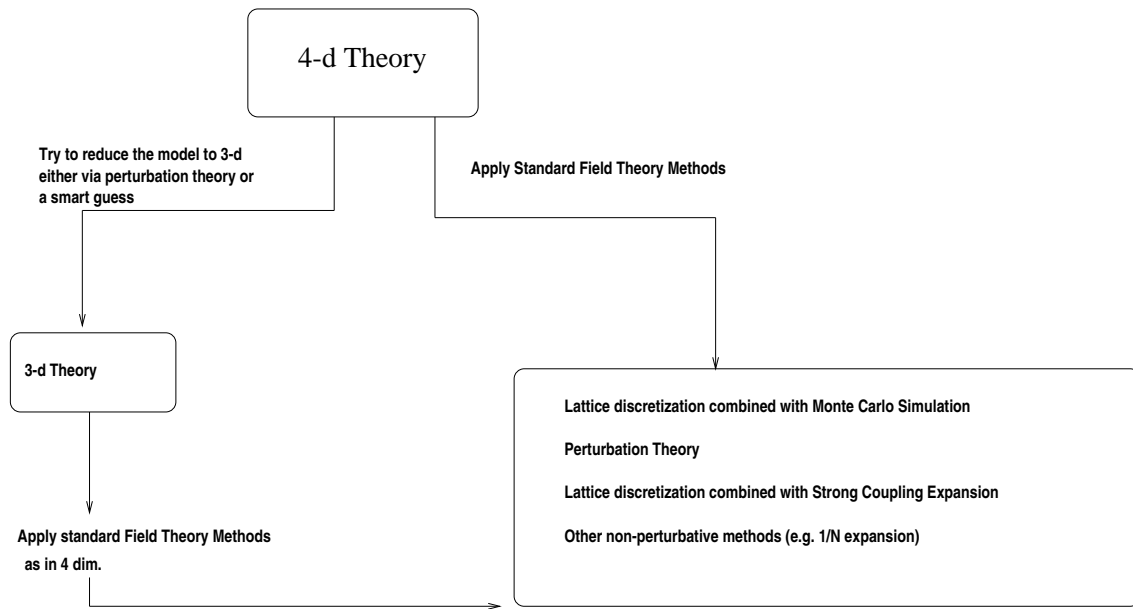


Figure 3: Calculational schemes for a 4d theory at a glance

In Figure 2.4 we give a sketch which outlines some of the various possibilities to calculate Z for a four dimensional model at finite T formulated in the imaginary time formalism.

Two remarks are in order. Firstly, the optimal strategy is model dependent and there is no general rule which can tell us a priori which is the best way to attack a problem. In the following we will see the various techniques at work in different models and situations.

Secondly, there are ideas which can be of general applicability. This is especially true for universality, for which a general framework is given by the symmetry analysis, breaking patterns and theory of critical phenomena. We then devote the next Section to a survey of this subject.

3 Critical Phenomena

The modern era of critical phenomena began about fifty years ago, when it was appreciated that very different fluids might well display *universal* behaviour: the coexistence curve, namely the plot of the reduced temperature T/T_c versus the reduced density ρ/ρ_c is the same! This observation has triggered important theoretical developments, in particular it has emerged that many phase transitions are associated with a spontaneous breakdown of some symmetry of the Hamiltonian, and that these symmetry changes can be triggered by temperature [22]. In this Section we briefly review main tools and ideas used in this field.

3.1 The Equation of State and the Critical Exponents

In a broad sense, the Equation of State is a relationship among different physical quantities characterising the critical state of a system, which only depend on a few parameters. For

instance for fluid systems it was soon realised that a general relationship describing the coexistence curve is:

$$(\rho - \rho_c) = A \left(\frac{T - T_c}{T_c} \right)^\beta \quad (27)$$

where T_c, ρ_c, A depend on the specific fluid under consideration, while the functional form above with $\beta \simeq 3$ holds true for all the fluids which have been studied.

It came then natural to apply the same idea to the critical phenomena in magnetic systems, identifying, in a completely heuristic way, the zero field magnetization M with the density difference:

$$M = A \left(\frac{T - T_c}{T_c} \right)^\beta \quad (28)$$

which can be easily generalised to include an external magnetic field h

$$\frac{h}{M^\delta} = f \left(\frac{T - T_c}{M^{1/\beta}} \right) \quad (29)$$

The above equation is the well known equation of state for magnetic systems, in one of its guises. For $h = 0$ we recover eq. (28), together with the definition of the exponent β . For $T = T_c$ we have

$$M = h^{1/\delta} \quad (30)$$

and we recognize that δ is the exponent describing the system's response at criticality. It is really remarkable that these definitions can be combined in just one relationship, the equation of state eq.(29). In short summary, then

- The Equation of State contains the usual definition of critical exponents (which is obtained by setting $h = 0$ or $T = T_c$)
- It gives information on the critical behaviour (i.e. the exponent δ) *also by working at $T \neq T_c$*
- It gives information on spontaneous magnetization (i.e. the exponent β) *also when there is an external magnetic field h*

The function f , in general, is unknown (it is possible to give some of its properties on general grounds [18]). It is useful to consider a first order expansion of the Equation of State

$$h = aM^\delta + b(T - T_c)M^{\delta-1/\beta} \quad (31)$$

which is more easily amenable to a direct comparison with data. Clearly, the range of applicability of eq.31 is smaller than the one of eq.29.

The idea outlined above can be applied in a broad range of context, including particle physics. We will discuss very many examples of this in the following, while in the following Table, as a first example, we summarize a 'dictionary' between magnetic systems, bosonic systems, and fermionic ones, where the order parameter is a composite fermion-antifermion condensate:

	Magnets	Bosons	Fermions
External Field	h (magnetic field)	m (bare mass)	m (bare mass)
Response Function	M (magnetization)	$\langle \sigma \rangle (m)$	$\langle \bar{\psi}\psi \rangle (m)$
Order Parameter	$M_0 = M(h = 0)$	$\langle \sigma \rangle (m = 0)$	$\langle \bar{\psi}\psi \rangle (m = 0)$

The systems above can be described in an unified way via the Equation of State we have discussed. Systems whose critical behaviour is characterised by the same exponents are said to belong to the same universality class. This circumstance is of course highly non trivial and it is rooted in the symmetries of the systems: systems whose critical behaviour is governed by the same global symmetries are in the same universality class. Strictly speaking this concept, as well as the equation of state itself, is limited to continuous transitions. Continuous transition have real divergencies, where the correlation length grows so large that it is possible to ignore all of the short range physics, but the one associated with the bosonic zero modes of the system. When this happens details of the dynamics do not matter any more, and the pattern of symmetries, their spontaneous breaking and realisation, drive the system's behaviour.

3.2 The Effective Potential

The Equation of State provides a macroscopic description of the order parameter of the system close to criticality. It is very useful and interesting to consider an intermediate level of description (in condensed matter/statistical physics it might be called mesoscopic) where the behaviour of the order parameter is inferred from its probability distribution (or for any distribution related with it). In turn, such probability distribution can/should be derived from the exact dynamics, with the help of a symmetries' analysis.

Main idea goes back to Landau, and is the following. One is supposed either to guess or to derive a function V_{eff} of the order parameter and external fields which describes the state of the system. We draw in Figure 3.2 the familiar plots showing V_{eff} as a function of the order parameter for several value of the external field (the temperature, for instance). The minimum of V_{eff} defines the most likely value of the order parameter, and so these plots determine the order parameter as a function of temperature. Also, for any give temperature we read off the plots wheater the system is in a pure state (just one minimum), or in a mixed phase (two non equivalent minima), which is only possible for a first order transition. In the upper plot we show the behaviour leading to a first order transition. For low temperature the system is in a phase characterised by a nonzero value of the order parameter. At $T = T^*$ (spinodal point) we have the first occurrence of a secondary minimum corresponding to a zero value of the order parameter, i.e. the onset of a mixed phase. For $T = T_c$ the two minima are equal, i.e. T_c is the critical point. Beyond T_c the minimum at zero is the dominant one. At $T = T^{**}$ the secondary minimum (for a nonzero value of the order parameter) disappears, and the mixed phase ends. In the lower diagram it is shown an analogous plot, but for a continuous (second order) transition. We note that a second order transition can be seen as a limiting case of a first order transition for $T^*, T^{**} \rightarrow T_c$.

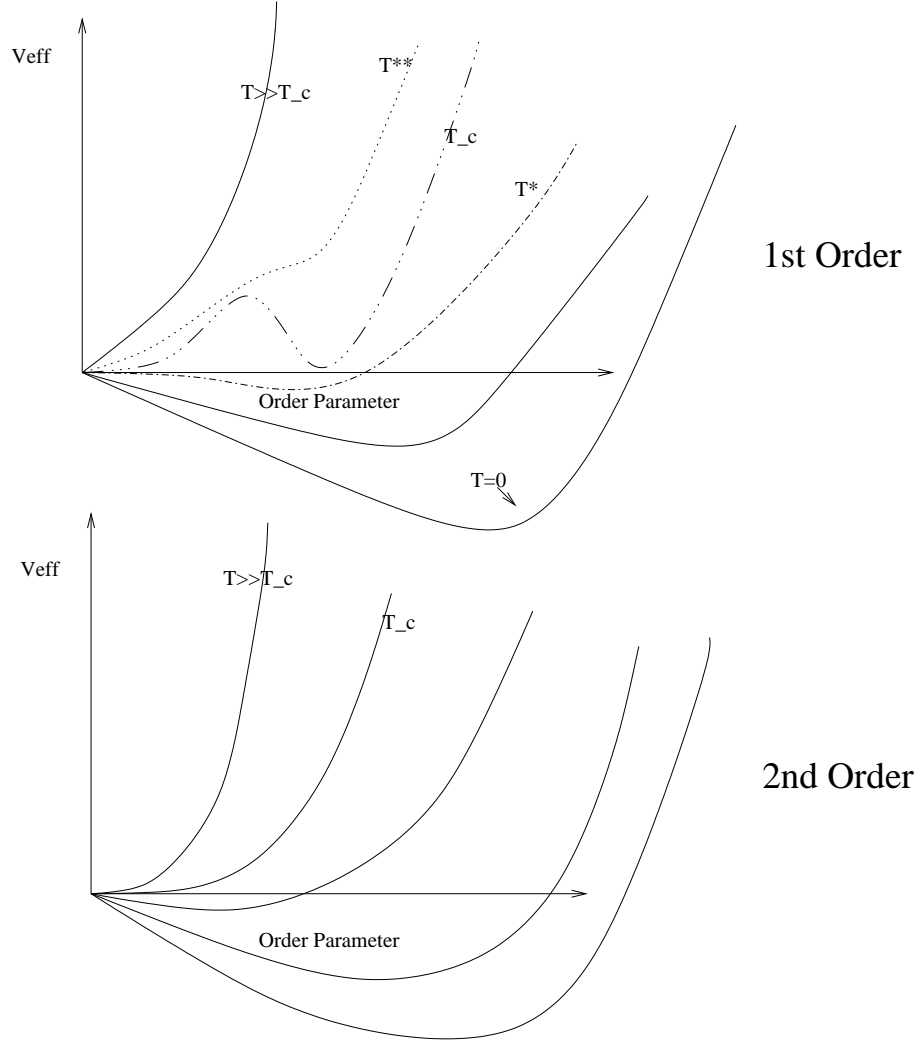


Figure 4: The shape of the effective potential for the order parameter for first order, discontinuous (upper diagram) and continuous transitions.

3.3 A Case Study

The idea discussed above can be nicely elucidated by the Potts model. There, one can find all possible examples of phase transitions, from continuous to discontinuous, and different intensities.

Consider the Action for the q -state two dimensional Potts model:

$$S = -\beta \sum \delta_{\sigma_i \sigma_j} \quad (32)$$

The spin variables σ can be in any of the q -possible states. The sum runs over nearest neighbors, and, for small β clusters of equal σ are preferred. When β increases there is a transition to a disordered state, for $\beta = \beta_c$.

The model has been analytically solved in a mean field approximation, where one can calculate β_c and the latent heat for any q . The latent heat turns out to be zero for $q \leq 4$,

corresponding to a second order transition, and positive, and increasing with q , for q larger than 4. For q very close to 4, the behaviour is *weakly first order* or nearly second order, in the sense that the first order transition behaves like a second order one, near, but not too near, the critical point. For instance, the inverse correlation length should obey the law

$$\xi^{-1} = A(\beta^* - \beta)^{\nu^*} \quad (33)$$

where β^* (to be identified with the T^* of the discussion above) and ν^* can be thought of as the coupling and critical exponent of the virtual second order transition point in the metastable region.

This behaviour has indeed been observed in numerical simulations, which can be described using the associated Ginzburg Landau model [19]. For instance the transition in the seven state Potts has a much smaller latent heat than the one with ten states, while the pseudocritical point β^* is much closer to β_c for $T = T_c$ for seven states than for ten.

One might think that the concept of a weak first order transition is a rather academic one. Indeed, it contrasts a bit with the familiar notion of an abrupt discontinuous transition, without precursor effects. It is then amusing to notice that a weak first order behaviour has been indeed observed not only in liquid crystals—the original de Gennes discussion on weak first order transitions— but also in the deconfining transition of Yang Mills model with $SU(3)$ color group—a transition which will be discussed at length in Section 7 – The strength of a first order transition is also an issue in the discussion of the electroweak transition [23], as we will review in the next Section.

3.4 Dynamical Symmetry Breaking

It is a fact that often the symmetries of the Hamiltonian are not realised in nature: for instance the complete translational invariance of a many body system is broken when the system becomes a crystal, or the chiral symmetry of the QCD Lagrangian is broken when quarks and antiquarks condense. The realisation, or lack thereof, of the symmetries of the Hamiltonian, i.e. the existence of different phases in a system, depends on the thermodynamic conditions. Hence, many phase transitions and critical phenomena are associated with a symmetry breaking/restoration[24].

One simple model to study this is the Goldstone model

$$L = (\partial_\mu \phi^\dagger)(\partial^\mu \phi) - V(\phi) \quad (34)$$

where ϕ is a complex scalar field and the potential $V(\phi)$ is given by

$$V(\phi) = 1/4\lambda(\phi^\dagger \phi - \eta^2)^2 \quad (35)$$

The Lagrangian is obviously invariant under $U(1)$ global phase transformation of the field ϕ . The only value of the field which realises such invariance is zero.

For positive λ and η^2 $V(\phi)$ has the well known Mexican hat shape: there is an infinity of minima of the effective potential for a nonzero value of the field. Once one particular minimum is selected, $\phi \neq 0$ and the symmetry is broken.

If η is tuned towards zero the global minima disappear, and the symmetry is restored: the only global minimum is the one corresponding to a zero value for the field.

It is worth noticing that simple models have also been used as toy models in various situations in particle, astroparticle or condensed matter physics: the nonrelativistic version of the Abelian Higgs model is identical to the Ginzburg-Landau model of a superconductor with ϕ representing the Cooper pair wave function, the Goldstone model describes the Bose condensation in superfluids, the σ model can be used to model the QCD high T phase transition, σ describing the composite $\langle \bar{\psi}\psi \rangle$ condensate, the three state Potts model models the deconfining transition in three color Yang-Mills, the spins representing the Polyakov loop, the non-Abelian Higgs model is used to study the electroweak transition, ϕ being in this case the Higgs field, etc. etc.

These toy models are amenable to approximate, mean field studies but to get real predictions one needs to study the full field theory from first principles. It is always very interesting to try to make contact between the exact results and those derived from simple models and analysis, so to assess the role of the quantum fluctuations. We will see examples of these points in the rest of these lectures, beginning with the electroweak transition in the next Section.

4 Electroweak Interactions at Finite Temperature

We want to know the fate of the spontaneously broken gauge symmetry of the electroweak interaction at high temperature. This depends on the value of the Higgs mass m_H , and cannot be solved within perturbation theory. This question has been successfully addressed by Laine, Kajantie, Rummukainen, Shaposhnikov in a series of papers [9] [10] [11] [7], and references therein. These authors have been using an admixture of perturbative dimensional reduction and lattice calculations, which eventually gives the phase diagram of the Electroweak sector of the Standard model in the m_H, T plane. A classical reference on the ElectroWeak transition and its phenomenological implications is [2].

The essence of the model can be found without inclusion of fermions. This is good news as, despite substantial progress in the formulation of chiral fermions on the lattice [25], practical calculations, at least in four dimensions, are still rather difficult. In addition to disregarding fermions, the effects of the U(1) group shall be neglected as well ($\sin^2\theta \simeq 0$), since its effects have been found to be small [10].

All in all, the Lagrangian we study is

$$L = 1/4 F_{\mu\nu}^a F_{\mu\nu}^a + (D_\mu \phi)^\dagger (D_\mu \phi) - m^2 \phi^\dagger \phi + \lambda (\phi^\dagger \phi)^2 \quad (36)$$

where ϕ is the Higgs doublet.

4.1 Perturbative Analysis

We begin by briefly reviewing the perturbative results, see [23] [14] [2] for details. Let us then build an effective potential from the electroweak Action by approximating the field $\hat{\phi}$ by a constant value ϕ , i.e. neglecting the fluctuations:

$$VT V_{eff}(\phi) = \int dt d^3x S(\hat{\phi}) \delta(\hat{\phi} - \phi) \quad (37)$$

The zero temperature tree level results reads is:

$$V_{eff}(\phi, T = 0) = -m^2/2\phi^2 + \lambda/4\phi^4 \quad (38)$$

(we can just consider the discrete $\phi \rightarrow -\phi$ symmetry which is enough to describe the behaviour of the order parameter).

The $T > 0$ one loop corrections basically are the effects of a non-interacting bose-fermi gas with frequencies depending on ϕ (the $-/+$; $+/-$ signs are for bosons/fermions):

$$V_{eff}^{1-loop}(\phi, T) = T \sum_i -/+ + \int \frac{d^3p}{(2p)^3} \ln \int 1 + / - e^{-(p^2 + \omega^2(\phi))^{1/2}/T} = \quad (39)$$

$$\frac{1}{2}\gamma\phi^2 T^2 \quad (40)$$

$$-\frac{1}{3}\alpha\phi^3 T \quad (41)$$

where both bosons and fermions contribute to the term in $\phi^2 T^2$, and the term in $\phi^3 T$ is from bosons alone. This yields:

$$V_{eff}(\phi, T) = -\frac{m^2}{2}\phi^2 + \frac{1}{2}\gamma T^2 - \frac{1}{3}\alpha T \phi^3 + \frac{1}{4}\lambda\phi^4 \quad (42)$$

$$= \frac{1}{2}\gamma(T^2 - T^{*2})\phi^2 - \frac{1}{3}\alpha T \phi^3 + \frac{1}{4}\lambda\phi^4. \quad (43)$$

We have defined $T^{*2} = m^2/\gamma$ and we will recognize that T^* is the pseudocritical point.

At $T = 0$ we have then the typical case of spontaneous symmetry breaking, with $\phi^2 = 2m^2/\lambda$. At 'large' T the positive quadratic term γT^2 dominates and symmetry is restored.

The cubic term drives the transition first order. The onset for metastability, i.e. of the mixed phase, coincides with the first appearance of a secondary minimum. It is then given by an inflexion point with zero slope:

$$\frac{\partial^2 V}{\partial \phi^2} = 0 \quad (44)$$

$$\frac{\partial V}{\partial \phi} = 0 \quad (45)$$

The solution is, as anticipated, $T = T^*$.

The critical temperature, from the equal minimum condition

$$V(\phi_1) = V(\phi_2) \quad (46)$$

is

$$T_c = T^* / \left(1 - \frac{2\alpha^2}{9\lambda\gamma}\right)^{1/2} > T^* \quad (47)$$

and it depends linearly on the Higgs mass:

$$T_c = m_H / \left(2\gamma - \frac{4\alpha^2}{9\lambda}\right)^{1/2} \quad (48)$$

As discussed in Section 3.3, the intensity of the transition is given either by the magnitude of the jump at T_c , $2\alpha/3\lambda$, and by the distance between T_c and T^*

$$T_c - T^* = T^* \left(1 / \left(1 - \frac{2\alpha^2}{9\lambda\gamma} \right)^{1/2} - 1 \right) \quad (49)$$

In conclusion the perturbative analysis of the electroweak model at high temperature predicts a first order transition. The transition weakens when $\alpha \rightarrow 0$ or $\gamma \rightarrow \infty$ or $\lambda \rightarrow \infty$, eventually becoming second order when the strength goes to zero and $T_c = T^*$ (cfr. again the behaviour of the Potts model [19]). Note that the quantum fluctuations are directly responsible for the weakening of the first order transition [23]. The complete inclusion of quantum fluctuations, which we are going to discuss, will cause the disappearance of the phase transition at large Higgs masses.

4.2 Four Dimensional Lattice Study

We know that in the electroweak sector of the Standard Model perturbation theory works well at zero temperature. As was pointed out in ref. [9] this is not true in general. It has been recognized that there are several scales in the problem. The smallest, which serves as a perturbative expansion parameter, is proportional to $g^2 T/m$, where m is any dynamically generated mass. Now, dynamically generated masses will be zero in the symmetric phase, hence perturbation theory will not be applicable there. And also in the broken phase, according to the intensity of the transition, perturbation theory might fail: when the transition is weakly first order, the mass approaches zero in the broken phase and perturbation theory is no longer reliable.

The exact approach uses ab initio lattice calculations on a four dimensional grid. These calculations are extremely expensive. The lattice spacing, which serves as an ultraviolet cutoff, must be smaller than the reciprocal of any physical energy scale: typically, at very high temperature, it must be smaller than $1/T$. On the other hand, the lattice size in space direction must be large enough to accommodate the lighter modes which are proportional to $1/g^2 T$, where g is the lattice coupling. As the continuum limit is found for $g \rightarrow 0$, also the requirement on size is quite severe.

In their numerical studies (see [7] for a review) the authors selected a few significant values for the Higgs mass, and studied the behaviour as a function of the temperature. The critical behaviour is assessed using the tools developed in statistical mechanics, finite size scaling of the susceptibilities, search for two states signal, etc. This analysis led to these results: for small values of the Higgs mass the 4-d simulations agree with perturbation theory, as expected. The first order line, which in perturbation theory weakens without disappearing, *ends* in reality, for an Higgs mass $\simeq 80 \text{ GeV}$. The discovery of such an endpoint [9] has been a major result, as it shows that there is no sharp distinction between the phases of the electroweak sector. The properties of this endpoint have been investigated in detail, confirming its existence, and placing it in the universality class of the 3d Ising model (a rather general results for endpoints).

4.3 Three Dimensional Effective Analysis

The main idea of the three dimensional effective analysis [11] is to use perturbation theory to eliminate the heavy modes, in the general spirit of dimensional reduction: this makes it definitely more easy to handle than the four dimensional theory. In the first place, three dimensions are of course cheaper than four. Secondly, and perhaps even most important, eliminating the heavy modes makes less severe the demand on lattice spacing. In conclusion, one can simulate the three dimensional theory on a much coarser lattice than the four dimensional one. The advantage over the four dimensional simulations is clear.

On the other hand, the three dimensional approach is much better than perturbation theory: we have noticed that perturbation theory cannot handle the light modes which might appear close to a (weak first order or second order) phase transition. Instead, the three dimensional model retain the light modes of the full model, only the heavy modes are integrated out.

But which model one should simulate? The model has the same functional form as the original one, i.e. it retains all of the particle content and symmetries:

$$L = \frac{1}{4}F_{\mu\nu}^a F_{\mu\nu}^a + (D_\mu\phi)^\dagger(D_\mu\phi) - m_3^2\phi^\dagger\phi + \lambda_3(\phi^\dagger\phi)^2 \quad (50)$$

where the subscript ‘3’ reminds us that we are working in three dimensions. The rule developed in [11] yields to an expression of (g_3, m_3, λ_3) in terms of the parameters of the four dimensional model. This is of course not trivial : for instance, in the three dimensional model there is no ‘obvious’ temperature dependence, as the fourth dimension has disappeared. All the temperature dependence is ‘buried’ in the parameters of the dimensionally reduced model.

The general arguments leading to the formulation, and applicability of the three dimensional effective theory are very convincing, but, as the authors pointed out, cross checks with the full four dimensional simulations are needed.

4.4 The Phase Diagram of the EW Sector of the Standard Model

In Figure 5, reproduced from the Laine-Rummukainen review of 1998 ref. [7], we see the phase diagram of the electroweak sector of the standard model, built by use and cross checks of the results obtained by the methods described above.

For small values of the Higgs mass $m_H < m_W$ the transition is strongly first order, and weakens (in the sense discussed in Section 3 above) when m_H increases. These results can be obtained in perturbation theory. For large Higgs mass ($m_H > m_W$) perturbation theory is no longer applicable, and a combination of lattice calculations of the four dimensional theory and of the (perturbatively reduced) three dimensional theory gives fully satisfactory results.

The endpoint was discovered in [9]. The nature and location of the second order endpoint, the most important result, has been actively investigated since then. From a phenomenological point of view, it is important to notice the transition ends at a value smaller than realistic Higgs masses.

The dotted line is the perturbative result reviewed in Section 4.1 : the limitation of the perturbative analysis is evident from the plot.

The fact that at small mass there is no phase transition, i.e. the discovery of the endpoint shows that there is no sharp distinction between the symmetric and broken phase of

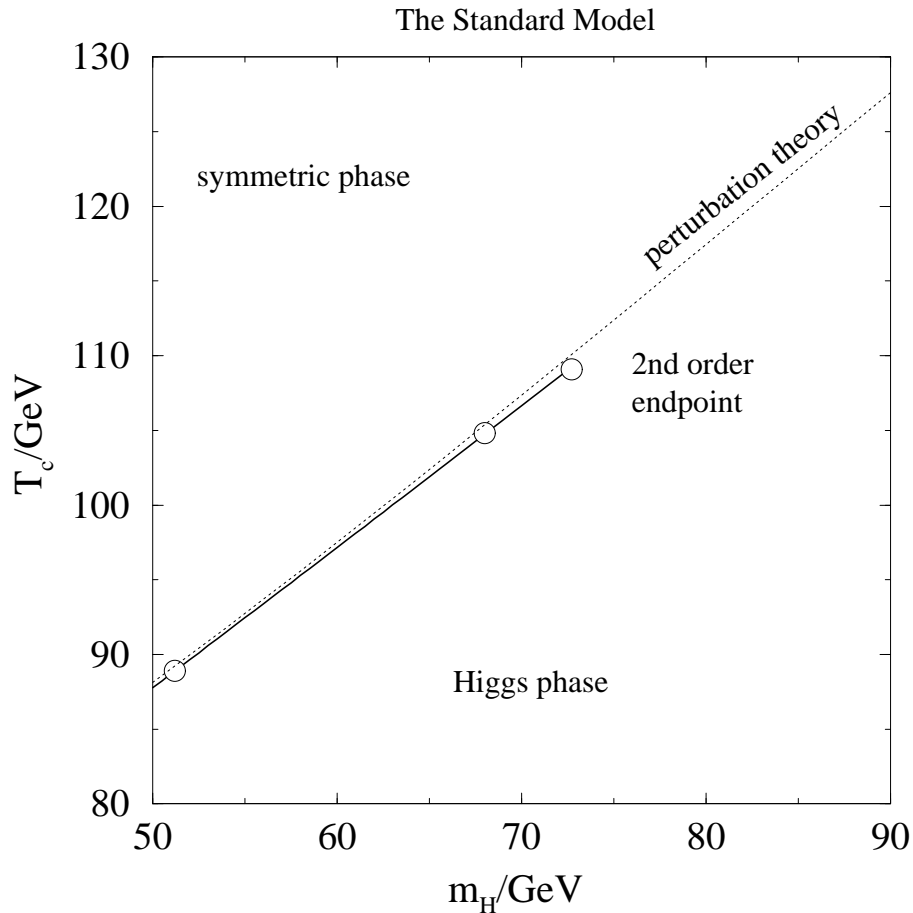


Figure 5: The phase diagram of the Electroweak Sector of the standard model in the temperature, Higgs mass plane, taken from Laine-Rummukainen [7]

the electroweak sector of the standard model, much like between liquid water and vapor. For instance, in principle massive W bosons in the broken phase cannot be distinguished from massive, composite objects in the symmetric phase.

Current research investigates the fate of these results in various supersymmetric extensions of the Standard Model [7] [8]. Of particular interest is the possibility that the line of first order phase transition continues up to realistic Higgs masses.

5 Thermodynamics of Four Fermions Models

Models discussed so far only included bosons. As a warmup for the study of Quantum Chromodynamics we discuss here purely fermionic models. Besides their illustrative value, such models can offer some insight into real QCD. In a nutshell, the idea is that the interaction between the massive quark can be described by a short range (in effect, contact) four-fermion interaction – to be specific, let us just remember the effective Lagrangian with the t’Hooft

instanton-mediated interaction:

$$\mathcal{L}_{\mathcal{I}} = K_I [(\bar{\psi}\psi)^2 + (\bar{\psi}i\gamma_5\vec{\tau}\psi)^2 - (\bar{\psi}\vec{\tau}\psi)^2 - (\bar{\psi}\gamma_5\psi)^2] \quad (51)$$

In the standard treatment of this effective Lagrangean spontaneous mass generation is imposed by fiat, and the resulting Lagrangean contains a mass term

$$\mathcal{L}_{eff} = \bar{\psi}(i\gamma^\mu D_\mu - m_\star + \mu\gamma_0)\psi - 1/4F_{\mu\nu}F^{\mu\nu} + \mathcal{L}_{int} \quad (52)$$

which explicitly breaks the global chiral symmetry of (51).

More generally, and perhaps more interestingly, fermionic models with a contact four fermion interaction display, in a certain range of parameters, spontaneous symmetry breaking and *dynamical* mass generation. They are thus a playground to study these phenomena in ordinary conditions, together with their fate at high temperature and density. This, besides being helpful to study QCD, it is also important from a more general point of view. A caveat is however in order before continuing: these models cannot describe confinement.

This section is devoted to the study of the thermodynamics of four fermion models with exact global chiral symmetry, see [26] [27] [28] [29] for early studies, reviews, details and recent developments. In a thermodynamics context, an important observation is that purely fermionic systems do not have zero modes, because of their antiperiodic boundary conditions. Hence, they are not amenable to direct dimensional reduction. We will see how the bosonised form of the models helps in this, and other respects. In particular, the bosonised form is amenable both to a simple mean field (large N) analysis, as well as to an exact lattice study. Let us also mention right at the onset, that these models (as opposed to QCD) can be studied exactly by means of lattice calculations also at nonzero density.

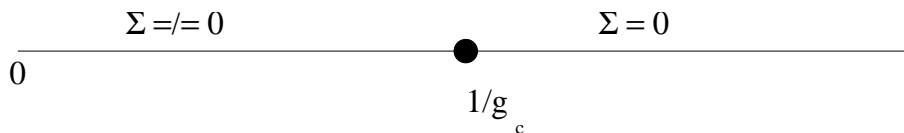


Figure 6: The phase diagram of the 3d Gross–Neveu model at $T = \mu = 0$. In the large coupling region the model has spontaneous symmetry breaking, and in that region is interesting to study the effects of temperature and chemical potential, which might have some similarity to QCD. The symmetric region is not relevant for thermodynamics.

To be specific, from now on we will concentrate on the 3dimensional Gross Neveu model, described by the Lagrangian

$$L = \bar{\psi}(\not{\partial} + m)\psi - g^2/N_f [(\bar{\psi}\psi)^2 - (\bar{\psi}\gamma_5\psi)^2] \quad (53)$$

The model is invariant under the chiral symmetries Z_2 and $U(1)$

$$\psi_i \rightarrow e^{i\alpha\gamma_5}\psi_i \quad (54)$$

$$\bar{\psi}_i \rightarrow \bar{\psi}_i e^{i\alpha\gamma_5} \quad (55)$$

The main properties of interest are:

- For large coupling, at $T = \mu = 0$, it displays spontaneous symmetry breaking, Goldstone mechanism and dynamical mass generation
- It has a rich meson spectrum, including a ‘baryon’ (infact, the fermion)
- It has a non-trivial (interacting) continuum limit
- It is amenable to an exact ab initio lattice study

As mentioned above, its analytic and numerical study is helped by auxiliary bosonic fields $\sigma, \vec{\pi}$. σ and $\vec{\pi}$ can be introduced by adding to \mathcal{L} the irrelevant term $(\bar{\psi}\psi + \sigma/g^2)^2 + (\bar{\psi}\gamma_5\psi + i\pi\gamma_5/g^2)^2$. \mathcal{L} then becomes (we set $m = 0$):

$$\mathcal{L} = \bar{\psi}(\not{\partial} + \sigma + i\pi\gamma_5)\psi + N_f/2g^2(\sigma^2 + \pi^2) \quad (56)$$

The continuous symmetry of the system is now reflected also by the rotation in the $(\sigma, \vec{\pi})$ chiral sphere.

A simple mean field analysis reveals the phase structure of the model at $T = \mu = 0$ which we sketch in Fig. 5. This is obtained by solving for the expectation value of the dynamical fermion mass $\Sigma \equiv \langle \sigma \rangle$ via the gap equation

$$\Sigma = g^2 \int_p \text{tr} \frac{1}{i/p + \Sigma} \quad (57)$$

yielding

$$\frac{1}{g^2} = - \int \frac{d^3p}{p^2 + \Sigma^2} \quad (58)$$

We find the solution $\Sigma \neq 0$, which breaks chiral symmetries, if

$$\frac{1}{g^2} < \frac{1}{g_c^2} = \frac{2\Lambda}{\pi^2} \quad (59)$$

(where Λ is the ultraviolet cutoff in the momentum integral above), hence the phase diagram of Fig.5

Consider now the effects of temperature or density, i.e. we ideally add another axes to the phase diagram of Fig. 5. If we start increasing temperature and density from the symmetric phase, things do not change much, while in the broken phase high temperature and/or density lead to the restoration of the chiral symmetries. This is intuitive if we just consider the disorder induced by temperature (of course the spins will become disordered in chiral space, not in the real one). This behaviour can be revealed by a mean field analysis. Let us first introduce explicitly temperature, as discussed in Sect. 2.3, by replacing the intergral over time by a sum over discrete Matsubara frequencies

$$\int d^3p \rightarrow \sum_{\text{Matsubara frequencies}} \int d^2p \quad (60)$$

and then include a chemical potential μ for baryon number N_b by adding to the Lagrangean a term μN_b :

$$\mu N_B \rightarrow \mu J_0 = \mu \bar{\psi} \gamma_0 \psi \quad (61)$$

(remember J_0 is the 0-th component of the conserved current $\bar{\psi}\gamma_\mu\psi$). All in all, the finite temperature–finite density generalisation of eq. 54 reads:

$$\frac{1}{g^2} = 4T \sum_{n=-\infty}^{n=+\infty} \int \frac{d^2p}{2\pi^2} \frac{1}{((2n-1)\pi T - i\mu)^2 + p^2 + \Sigma^2(\mu, T)} \quad (62)$$

We can now eliminate the coupling in favour of $\Sigma_0 = \Sigma(T=0, \mu=0)$

$$\Sigma - \Sigma_0 = -T[\ln(1 + e^{-(\Sigma-\mu)/T}) + \ln(1 + e^{-(\Sigma+\mu)/T})] \quad (63)$$

This gives the behaviour of the order parameter at fixed temperature as a function of μ . A chiral restoring phase transition is apparent for any temperature. At $T=0$ the transition is (very strongly) first order, and occurs for $\mu_c = m_F(\mu=0)$, as expected of simple models. For any other temperature the transition is second order, and μ_c gets smaller and smaller while increasing the temperature, eventually becoming 0 at $T = T_c$. A similar calculation gives the equation of state, in particular for $T=0$ the baryon number N_b is seen to (approximatively) follow the prediction of a free (massless) fermion gas $N_b \propto \mu^3$. The behaviour of the order

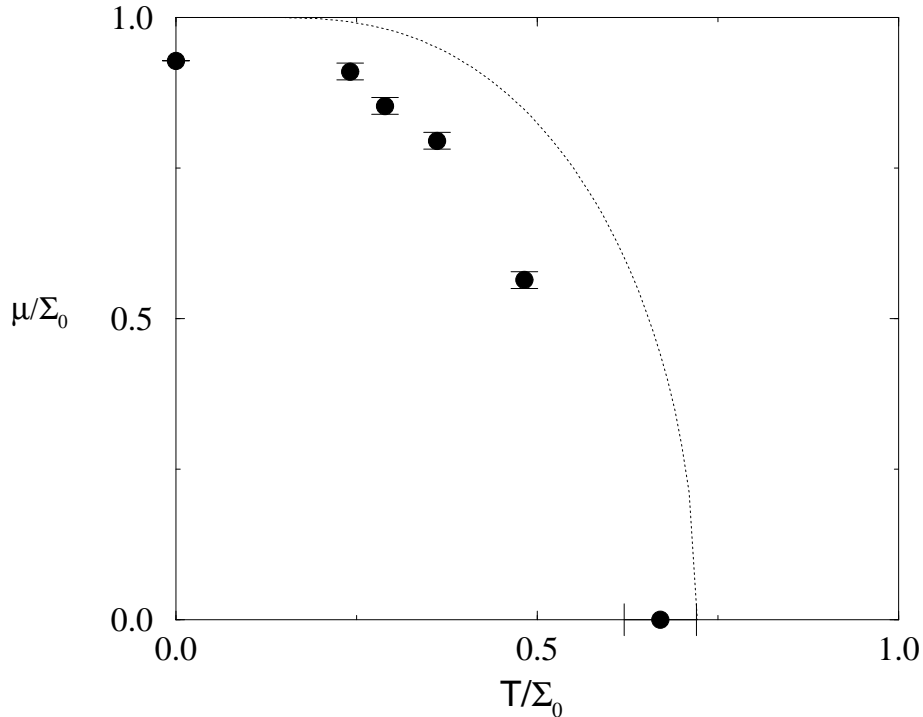


Figure 7: The phase diagram of the 3d Gross–Neveu model in the T, μ plane. The coupling has been selected in such a way that the model is in the symmetry broken phase at $T = \mu = 0$. Chiral symmetry restoration at large T, μ is observed either in mean field calculation (solid line) and exact lattice simulations (points). Taken from S. Hands, ref. [28]

parameter can be used to draw the phase diagram in the temperature–chemical potential plane, Figure 5

But what happens beyond mean field? Or, equivalently, what happens when the number of flavor decreases from infinite to any finite number? (the results of the mean field analysis can be shown to be equivalent to the leading order of a $1/N_f$ expansion). Although it is possible to calculate $1/N_f$ corrections it is clearly desirable to have some exact results. For instance, one wants to find out exactly the position of the tricritical point where the first order line merges with the second order one (mean field predicts $\mu = 0$). Or, one might inquire about the stability of the nuclear matter phase, i.e. for which range of temperature one can excite massive fermions, before restoring the chiral symmetry? These and other points have been studied in [29]: the authors have shown that dimensional reduction is valid at the finite T transition, discussed the existence of a tricritical point and the possibility of a nuclear liquid–gas transition. Clearly these aspects depend on the exact dynamics. We have seen in the discussion on the electroweak transition that mean field can give completely misleading indications. A feeling about the relevance of the quantum corrections in this model can be obtained by comparing the phase diagram obtained on the lattice, and via the mean field calculation described here (see Figure 7) : we note that there is no qualitative change, however there are sizeable differences.

Let us summarize: the phase diagram of four fermion models can be studied within a self consistent mean field approach, equivalent to a leading order expansion in $1/N_f$. These models are amenable to an exact lattice study (at variance with QCD whose lattice study, as we shall see, is limited to $\mu = 0$). The results available on the lattice, while confirming many qualitative trends, show also significant deviations from a simple mean field analysis. Going from simple calculations of simple models to exact calculations of the same models can give interesting, new information, and much is still to be done in this field.

6 The Phases of QCD

Let us recall the symmetries of the QCD action with N_f flavors of massless quarks, coupled to a $SU(N_c)$ color group:

$$SU(N_c)_C \times SU(N_f) \times SU(N_f) \times Z_A(N_f) \quad (64)$$

$SU(N_c)$ is the gauge color symmetry. $SU(N_f) \times SU(N_f) \times Z_A(N_f)$ is the flavor chiral symmetry, after the breaking of the classical $U_A(1)$ symmetry to the discrete $Z_A(N_f)$.

We want to study the realisation and pattern(s) of breaking of the chiral symmetries and we would like to know the interrelation of the above with the possibility of quark liberation predicted at high temperature and density[31].

The first task – fate of the chiral symmetries – is made difficult by the problems with simulating QCD with three colors at finite baryon density. Aside from this, the tools for investigating the transition are all at hand: significant results at finite temperature have been obtained from first principle calculations on the lattice, while the phase diagram of the two color model (which can be simulated at nonzero baryon density) is well underway. For a recent phenomenological approach to finite density QCD, not discussed here, we refer again to [13]. The second task – confinement – poses more conceptual problems. It can be addressed satisfactorily only in Yang Mills systems, which enjoy the global $Z(N_c)$ symmetry of the center of the gauge group. When light quarks enter the game, the global $Z(N_c)$

symmetry is lost, and the simple description of confinement in terms of such symmetry is not possible any more.

In normal condition (zero temperature and density) the $SU(N_f)_L \times SU(N_f)_R$ chiral symmetry is spontaneously broken to the diagonal $SU(N_f)_{L+R}$. This should be signaled by the appearance of a Goldstone boson, and a mass gap. In the real world, as such a symmetry is only approximate, the would be Goldstone is not exactly massless, but it is nevertheless lighter than any massive baryon –i.e. there is a ‘relic’ of the mass gap. All of them can be described by chiral perturbation theory, where the small expansion parameter is, essentially, the bare quark mass.

Most dramatic dynamical features of QCD are confinement and asymptotic freedom: in ordinary condition quarks are ‘hidden’ inside hadrons, i.e. all the states realised in nature must be color singlet. If one tries to ‘pull’ one quark and one antiquark infinitely apart, the force between them grows with distance—which is also called infrared slavery. At short distance, instead, quarks are nearly free: this is called asymptotic freedom.

In summary, these are the features of QCD we shall be concerned with in the next two Sections:

- Asymptotic freedom
- Confinement
- Spontaneous chiral symmetry breaking

Confinement and realisation of chiral symmetry depend on the thermodynamic conditions, and on the number of flavors and colors. Asymptotic freedom does not depend on thermodynamics: it holds true till

$$N_f < 11/2N_c \tag{65}$$

For $T = \mu = 0$ there is then a line (see Fig. 6) in the N_c, N_f plane separating the ‘ordinary’ phase of QCD from one without asymptotic freedom. More exotic phases have been predicted as well [36], but it is anyway well established that it does exist a region in the N_f, N_c plane which is characterised by confinement, spontaneous chiral symmetry breaking and asymptotic freedom. The third axes can represent either temperature and density: one might well imagine that the any point belonging in the same sector of the phase diagram in Fig. 6 would behave in a similar way while increasing temperature and density. It is then interesting to study the thermodynamics of models with different N_c and N_f , looking for similarities and differences.

In the discussion of the next two Sections we will consider $N_c = 3$, the real world, and $N_c = 2$, for technical reasons, and because it represents an interesting limiting case. We will discuss the Yang Mills model, which also describes QCD with quarks of infinite mass. We will mostly discuss two light flavors, which is rather realistic, as the up and down quarks are much lighter than any other mass. Understanding the behaviour with three flavor is important as well, as in the end the real world is somewhere in between $N_f = 2$ and $N_f = 3$.

7 QCD at Finite Temperature, $\mu_B = 0$

Disorder increases with temperature. Then, one picture of the high T QCD transition can be drawn by using the ferromagnetic analogy of the chiral transition mentioned in Section 2:

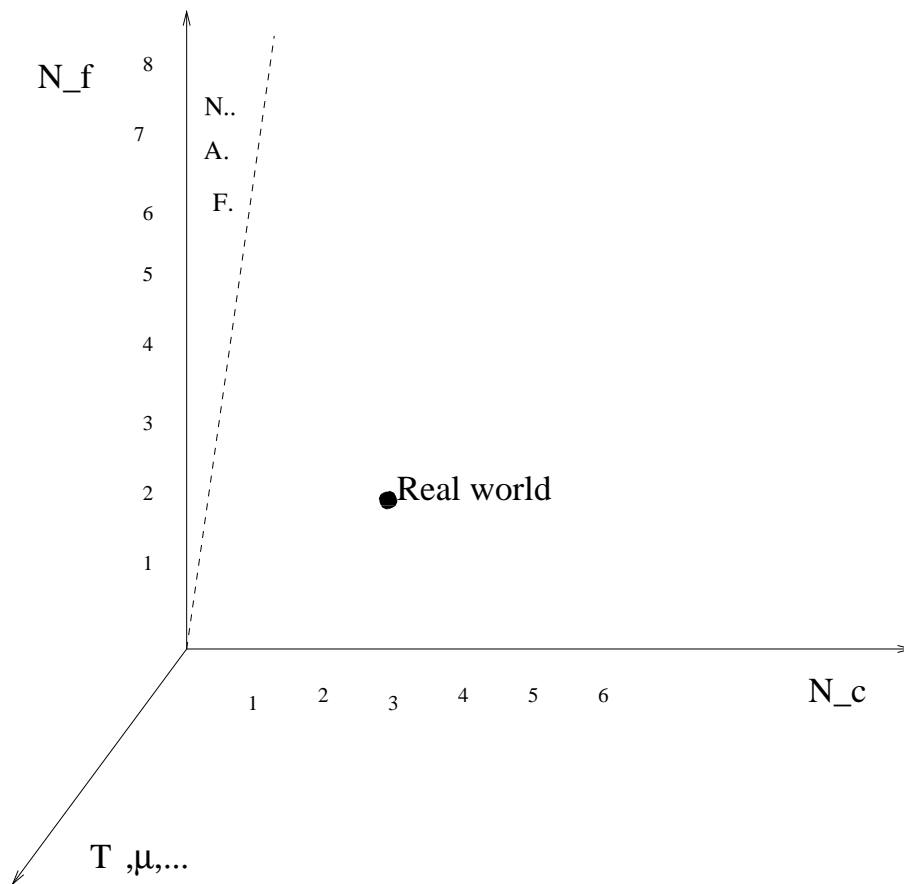


Figure 8: The phase diagram QCD in the N_f , N_c , and thermodynamic parameters space. The everyday world corresponds to $N_c = 3$, $N_f = 2$ (approximately), $T = \mu = 0$. For $T = \mu = 0$ there is a line in the N_c, N_f plane separating the ‘ordinary’ phase of QCD from one without asymptotic freedom.

$\bar{\psi}\psi$ can be thought of as a spin field taking values in real space, but whose orientation is in the chiral sphere. Chiral symmetry breaking occurs when $\langle \bar{\psi}\psi \rangle \neq 0$, i.e. it corresponds to the ordered phase. By increasing T , $\langle \bar{\psi}\psi \rangle \rightarrow 0$. This is very much the same as in the Gross Neveu model of Section 5. Color forces at large distance should decrease with temperature: the main mechanism, already at work at $T = 0$, is the recombination of an (heavy) quark and antiquark with pairs generated by the vacuum: $\bar{Q}Q \rightarrow \bar{q}Q + q\bar{Q}$. At high temperature it becomes easier to produce light $\bar{q}q$ pairs from the vacuum, hence it is easier to ‘break’ the color string between an (heavy) quark and antiquark $\bar{Q}Q$. In other words, we expect screening of the color forces. It is however worth mentioning that, even if the string ‘breaks’ bound states might well survive giving rise to a complicated, non-perturbative dynamics above the critical temperature. The physical scale of these phenomena is the larger physical scale in the system, i.e. the pion radius (cfr. the discussions in Section 2).

There are two important limits which are amenable to a symmetry analysis : $m_q = 0$ and $m_q = \infty$.

7.1 QCD High T P.T., and Symmetries I : $m_q = 0$ and the Chiral Transition

When $m_q = 0$ the chiral symmetry of eq.(64) is exact. As both m_u and m_d are much smaller than Λ_{QCD} , this is a reasonable approximation. Note the isomorphy

$$SU(2) \times SU(2) \equiv O(4) \tag{66}$$

which shows that the symmetry is the same as the one of an $O(4)$ ferromagnet. The relevant degrees of freedom are the three pions, and the sigma particle, and the effective potential is a function of $\sigma^2 + |\pi|^2$ in the chiral space. Once a direction in the chiral sphere is selected (say in the σ direction) chiral symmetry is spontaneously broken in that direction, according to the pattern: equivalently

$$SU(2)_R \times SU(2)_L \rightarrow SU(2)_{L+R} \tag{67}$$

$$O(4) \rightarrow O(3) \tag{68}$$

Massless Goldstone particles (in this case, the three pions) appear in the direction orthogonal to the one selected by the spontaneous breaking.

Combining this symmetry analysis with the general idea of dimensional reduction, Pisarski and Wilczek [20] proposed that the high temperature transition in the two flavor QCD should be in the universality class of the $O(4)$ sigma model in three dimensions. At high temperature when symmetry is restored there will be just one global minimum for zero value of the fields, and pion and sigma become eventually degenerate.

We have however to keep in mind possible sources of violation of this appealing scenario (see [37] for recent discussions).

Firstly, is the very nature of the symmetry which is restored across the transition. [20] [38] Note infact that the σ model picture assumes that the axial $U(1)$ symmetry remains broken to $Z(N_f)$ across the phase transition, in such a way that it does not impact on the critical behaviour. This is indeed a dynamical question – which symmetry is restored first – which can only be answered by an ab initio calculation.

One second possible source of violation of this scenario relates with a strong deconfining transition happening for its own reasons. Such deconfining transition would liberate abruptly an huge amount of degrees of freedom, and would likely trigger also the restoration of chiral symmetry. In this case, the chiral transition would be hardly related with the sigma model.

And there are also practical considerations: maybe the scenario is true, but the scaling window is so small that it has no practical applicability or relevance. One example of this behaviour is offered by the $Z(N_f) \times Z(N_f)$ 3 dimensional Gross-Neveu model. Its high T phase transition should be in the universality class of the Ising model, but the scaling window turns out to be only $1/N_f$ wide, i.e. it shrinks to zero in the large N_f (mean field) limit, in which case dimensional reduction is violated.

All in all, one has to resort to numerical simulations to measure the critical exponents, and verify or disprove the $O(4)$ universality. In turn, this gives information on the issues (nature of the chiral transition, role of deconfinement, heavy modes decoupling, etc.) raised above.

In practice, one measures the chiral condensate as a function of the coupling parameter β , which in turns determines the temperature of the system. This gives the exponent β_{mag} (remember the discussions in Section I) according to

$$\langle \bar{\psi}\psi \rangle = B(\beta - \beta_c)^{\beta_{mag}} \quad (69)$$

The exponent δ is extracted from the response at criticality:

$$\langle \bar{\psi}\psi \rangle = Am^{1/\delta}; \beta = \beta_c \quad (70)$$

The results (we quote only ref. [37] as there is a substantial agreement) : $\beta_{mag} = .27(3)$, $\delta = 3.89(3)$ compare favourably with the O(4) results $\beta_{mag} = .38(1)$, $\delta = 4.8(2)$, and definitively rule out mean fields exponents (which would have characterised a weak first order transition). However, the results can still be compatible with O(2) exponents, which would signal the persistence of some lattice artifact, $\beta_{mag} = .35(3)$, $\delta = 4.8(2)$, and of course it is still possible that the final answer do not fit any of the above predictions, for instance one is just observing some crossover phenomenon.

7.2 Two Color QCD I

Two color QCD enjoys an enlarged (Pauli–Gürsey) chiral symmetry: quarks and antiquarks belong to equivalent representation of the color group (see for instance the first entry of [47], and references therein) . As a consequence of that the ordinary chiral symmetry of QCD

$$SU(N_f) \times SU(N_f) \quad (71)$$

is enlarged to $SU(2N_f)$. The spontaneous breaking of $SU(2N_f)$ then produces a different pattern of Goldstone bosons, which includes massless baryons (diquarks). The relevant sigma model in this case includes also diquarks and antidiquarks. Because of this symmetry, we have an exact degeneracy of the pion, scalar qq and scalar $\bar{q}\bar{q}$ and of the scalar meson, pseudoscalar qq and pseudoscalar $\bar{q}\bar{q}$: this is precisely the reason why we have massless baryons in the model, and thus why this is not, a priori, a good guidance to QCD at finite baryon density (to be discussed in Section 8).

The Pauli–Gürsey symmetry has implications on the universality class of the chiral transition at high temperature: for instance, the predictions of universality+dimensional reduction for the two color, two flavour is $O(6)$ critical exponents [39]. The general argument is clear, but it has been fully appreciated and studied only recently. Also, this tells us that qualitative arguments relating the universality class of the chiral transition to the flavour, but not to the color group, have to be used with care: at least for two color QCD, which is an interesting limit case, the number of color matters for the high temperature chiral transition as well.

7.3 QCD High T p.t., and Symmetries II : $m_q = \infty$ and the Confinement Transition

When $m_q = \infty$ quarks are static and do not contribute to the dynamics : hence, the dynamic of the system is driven by gluons alone, i.e. we are dealing with a purely Yang-Mills model:

$$S = F_{\mu\nu}F^{\mu\nu} \quad (72)$$

In addition to the local gauge symmetry, the action enjoys the global symmetry associated with the center of the group, $Z(N_c)$. The order parameter is the Polyakov loop P

$$P = e^{i \int_0^{1/T} A_0 dt} \quad (73)$$

In practice, P is the cost of a static source violating the $Z(N_c)$ global symmetry.

The interquark potential $V(R,T)$ (R is the distance, T is the temperature) is

$$e^{-V(R,T)/T} \propto \langle P(\vec{0})P^\dagger(\vec{R}) \rangle \quad (74)$$

Confinement can then be read off the behaviour of the interquark potential at large distance. When $V(R) \propto \sigma R$ it would cost an infinite amount of energy to pull two quarks infinitely apart. Above a certain critical temperature $V(R)$ becomes constant at large distance: i.e. the string tension is zero, confinement is lost. The implication of this is that $|P|^2 = V(\infty, T)$ is zero in the confining phase, different from zero otherwise. P plays thus a double role, being the order parameter of the center symmetry, and an indicator of confinement (for an alternative symmetry description of the pure gauge deconfinement transition see [40]). We learn that in Yang Mills models there is a natural connection between confinement and realisation of the $Z(N_c)$ symmetry. Hence, the confinement / deconfinement transition in Yang Mills systems is amenable to a symmetry description. By applying now the same dimensional reduction argument as above, we conclude that the Universality class expected of the three color model is the same as the one of a three dimensional model with $Z(3)$ global symmetry: this is the three state Potts model discussed in Section 3.3. Indeed, the transition turns out to be ‘almost’ second order, i.e. very weakly first order, like the 3d three state Potts model, see [41] for review and phenomenological implications of this observation.

7.4 Two Color QCD II

The same reasoning tells us that the two color model is in the universality class of the three dimensional $Z(2)$ (Ising) model. This prediction has been checked with a remarkable precision [21], and it is a spectacular confirmation of the general idea of universality and dimensional reduction.

Source		$SU(2)$	Ising
$\langle L \rangle$	β/ν	0.525(8)	0.518(7)
$D \langle L \rangle$	$(1 - \beta)/\nu$	1.085(14)	1.072(7)
	$1/\nu$	1.610(16)	1.590(2)
	ν	0.621(6)	0.6289(8)
	β	0.326(8)	0.3258(44)
χ_ν	γ/ν	1.944(13)	1.970(11)
$D\chi_\nu$	$(1 + \gamma)/\nu$	3.555(15)	3.560(11)
	$1/\nu$	1.611(20)	1.590(2)
	ν	0.621(8)	0.6289(8)
	γ	1.207(24)	1.239(7)
	$\gamma/\nu + 2\beta/\nu$	2.994(21)	3.006(18)
g_r	$-g_r^\infty$	1.403(16)	1.41
Dg_r	$1/\nu$	1.587(27)	1.590(2)
$(\omega = 1)$	ν	0.630(11)	0.6289(8)

Taken from J. Engels, S. Mashkevich, T. Scheideler and G. Zinovjev, ref. [21]

7.5 Summary and Open Questions for the QCD High T Transition

In Figure 7 we sketch a phase diagram in the temperature, bare mass plane for a generic version of QCD with N_f flavor degenerate in mass, and N_c color.

For zero bare mass the phase transition is chiral. For three colors, two flavors is second order with $T_c \simeq 170 \text{ Mev}$. The prediction from dimensional reduction + universality – $O(4)$ exponents – is compatible with the data, but the agreement is not perfect. If the agreement were confirmed, that would be an argument in favour of the non-restoration of the $U_A(1)$ symmetry at the transition, which is also suggested by the behaviour of the masses spectrum. Remember infact that the chiral partner of the pion is the f_0 , which is in turn degenerate with the scalar a_0 with $U_A(1)$ is realised. All in all, $U_A(1)$ non-restoration across the chiral transition corresponds to $m_\pi \simeq m_{f_0} \neq m_{a_0}$ which is the pattern observed in lattice calculations [34]. The transition with three (massless) flavour turns out to be first order. The question is than as to whether the strange quark should be considered ‘light’ or heavy’. In general, the real world will be somewhere in between two and three light flavour, and to really investigate the nature of the physical phase transition in QCD one should work as close as possible to the realistic value of the quark masses.

By switching on the mass term chiral symmetry is explitley broken by $m < \bar{\psi}\psi >$. In the infinite mass limit QCD reduces to the pure gauge (Yang Mills) model. Yang Mills systems have a deconfining transition associated with the realisation of the global $Z(N_c)$ symmetry. This places the system in the Ising 3d universality class for two colors, and makes the transition weakly first order (near second, infact) for three colors. General universality arguments are perfectly fulfilled by the deconfining transition.

The $Z(N_c)$ symmetry is broken by the kinetic term of the action when the quarks are dynamic ($m_q < \infty$): this particular symmetry description of deconfinement only holds for infinite quark mass. Till very recently then the most convincing signals for deconfinement with dynamical quarks come from the equation of state. For instance the behaviour of the internal energy is a direct probe of the number of degeres of freedom, and indicates quark and gluon liberation [34].

Another important set of information come from the behaviour of the mass spectrum – this is of course every relevant both on experimental grounds, for the ungoing RHIC experiments as well as for the upcoming ones, as well as for completing our understanding of patterns of chiral symmetry. The most dramatic phenomena , i.e the disappearance of the Goldstone mode in the symmetric phase, the nature of the Goldstone mechanism in four fermion models, as well as the massive fermion in the broken one, have been already studied on the lattice.

Among the most prominent open questions, there is of course the behaviour of ‘real’ QCD, with two light flavour, and a third one of the order of Λ_{QCD} , so how and when exactly the $N_f = 2$ scenario morfs with the $N_f = 3$? Also, why is T_χ much smaller that the pure gauge deconfining transition? At a theoretical level the question is if it is possible to give an unified description of the two transitions, chiral and deconfining. This question is currently under active investigation: recent work suggests that a symmetry analysis of the deconfining transition can be extended also to theories with dynamical fermions. The physical argument is rooted in a duality transformation which allows the identification of magnetic monopoles as agent of deconfinement. The order parameter for deconfinement

would that be the monopole condensate [32]. An alternative approach uses percolation as the common agent driving chiral and confining transitions [33].

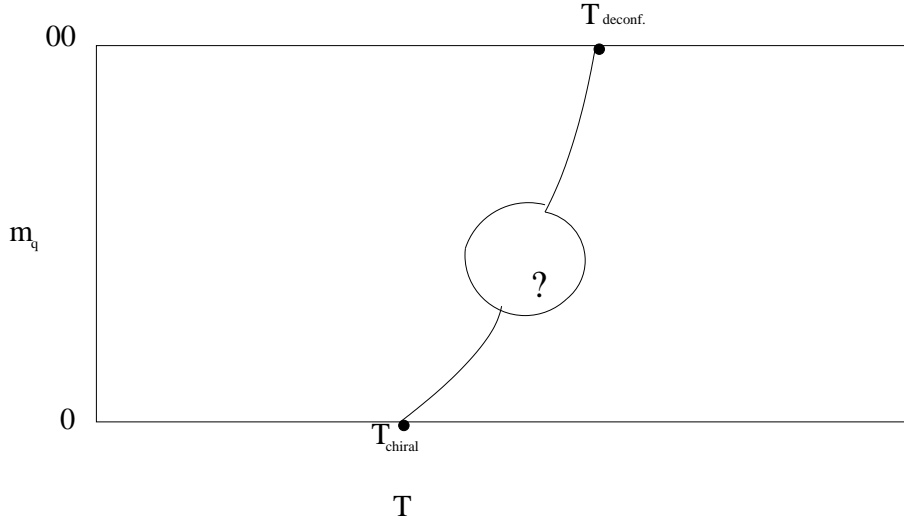


Figure 9: The ‘phase diagram’ QCD in the quark mass, temperature plane—see text.

8 QCD at Finite Temperature, $\mu_B \neq 0$

Let us now consider the effects induced by an increased baryon density, when baryons start overlapping. The most natural prediction relates with asymptotic freedom: as the quarks get nearer and nearer they do not feel the interactions any more, whilst the long range interaction is screened by many body effects. The natural conclusion is that the system is ‘nearly free’ (i.e. non confining) hence chiral symmetry is realised (one needs some interaction to break the symmetry of the action). Both on physical grounds, and from the predictions of simple models (Gross–Neveu, Section 5) we expect the typical scale of critical phenomena at finite density to be set by the lighter particle carrying baryon number.

First principle calculations should be able to confront these predictions, as well as results obtained by use of semi-approximate calculations of symmetry motivated models [13] and to put them on firm quantitative grounds.

We address here three main points:

- Why is QCD at finite density difficult
- What do we know from first principles
- What can we do, in practice

The critical region of QCD is outside the reach of perturbative calculations, then one should use ab initio lattice methods. As most people have already heard, this is plagued by several problems. To understand the problems, and to propose some solution, or, at least, workaround, we have now to give some (quick) detail of these calculations.

Consider again the partition function:

$$\mathcal{Z}(\mu, T) = \int_0^{1/T} dt \int e^{S(\bar{\psi}, \psi, U)} d\bar{\psi} d\psi dU \quad (75)$$

A chemical potential for baryons is introduced by adding the term μJ_0 , where $J_0 = \bar{\psi} \gamma_0 \psi$ is the 0th component of the conserved particle number current. In momentum space, this corresponds to the substitution $p_0 \rightarrow p_0 - i\mu$.

Let us now specialise to the QCD Action

$$S_{QCD} = F_{\mu\nu} F_{\mu\nu} + \bar{\psi} (\not{D} + m + \mu\gamma_0) \psi = S_G + \bar{\psi} M \psi \quad (76)$$

and exploit the bilinear form of the fermionic part of the Action to integrate explicitly over the fermions. This yields:

$$\mathcal{Z}(T, \mu) = \int dU \det M e^{-S_G} = \int dU e^{-(S_G - \log(\det M))} \quad (77)$$

The partition function can be *exactly* written in terms of an Action which only contains gauge field, $S_{eff} = S_G - \log(\det M)$ (we often call it an effective Action, however we should remember that no information has been lost in its definition)

Once the model is formulated on a lattice, one can express the integral over space as a sum over the lattice sites, and the relevant observables can be calculated by use of the importance sampling. For this to be viable, S_{eff} should be real. The problem is that for three colors QCD S_{eff} is not real.

The usual numerical methods then cannot be applied. Alternative methods which have been proposed so far fail at zero temperature, but could be applied, maybe, at nonzero temperature [42]. Interesting new idea have been proposed, and tested in spin models [43]. All this is promising and gives some hope that at least the region around T_c , small chemical potential can be understood in the near future, see [43] for a review on recent efforts.

There is however something else one can try within the lattice formalism, which is the subject of the next subsection.

8.1 The Lattice Strong Coupling Analysis of the QCD Phase Diagram

The lattice formulation, besides being suited for statistical MonteCarlo simulations, lends also itself to an elegant expansion in terms of the inverse gauge coupling ([45] [46]). As the continuum limit (i.e. real QCD) corresponds to zero gauge coupling, at a first sight one might think that the so-called strong coupling expansion is hopeless. But there is a very important point: for two or three color QCD there are no phase transitions as a function of coupling. Hence, many qualitative features - most important, confinement and chiral symmetry breaking - do not depend on the gauge coupling itself. Moreover, this expansion is systematically improvable: it is worth noticing a nice work where the asymptotic scaling associated with the continuum limit was reached from strong coupling [44]!!

Another interesting feature is that the strong coupling expansion yields a purely fermionic model, with four fermion interactions. Then, the strong coupling expansion can also be seen as a tool for deriving effective models for QCD from an ab initio formulation.

The starting point is the QCD lattice Lagrangean:

$$\begin{aligned}
S = & -1/2 \sum_x \sum_{j=1}^3 \eta_j(x) [\bar{\chi}(x) U_j(x) \chi(x+j) - \bar{\chi}(x+j) U_j^\dagger(x) \chi(x)] \\
& -1/2 \sum_x \eta_0(x) [\bar{\chi}(x) U_0(x) \chi(x+0) - \bar{\chi}(x+0) U_0^\dagger(x) \chi(x)] \\
& -1/3 \sum_x 6/g^2 \sum_{\mu,\nu=1}^4 [1 - reTr U_{\mu\nu}(x)] \\
& + \sum_x m \bar{\chi} \chi
\end{aligned} \tag{78}$$

The $\chi, \bar{\chi}$ are the staggered fermion fields living on the lattice sites, the U 's are the $SU(N_c)$ gauge connections on the links, the η 's are the lattice Kogut–Susskind counterparts of the Dirac matrices, and the chemical potential is introduced via the time link terms $e^\mu, e^{-\mu}$ which favour (disfavour) propagation in the forward (backward) direction thus leading to the desired baryon-antibaryon asymmetry.

We have written down explicitly the lattice Action to show that the pure gauge term $S_G = -1/3 \sum_x 6/g^2 \sum_{\mu,\nu=1}^4 [1 - reTr U_{\mu\nu}(x)]$ contain the gauge coupling in the denominator, hence it disappears in the infinite coupling limit. Consequently, one can perform independent spatial link integration, leading to

$$\mathcal{Z} = \int \prod_{timelinks} dU_t d\bar{\chi} d\chi e^{-1/4N \sum_{\langle x,y \rangle} \bar{\chi}(x) \chi(x) \bar{\chi}(y) \chi(y)} e^{-S_t} \tag{79}$$

where $\sum_{\langle x,y \rangle}$ means sum over nearest neighboring links, terms of higher order have been dropped, and we recognize a four fermion interaction. From there on things proceed formally much in the same way as for the Gross-Neveu model discussed in Section 5, and we quote the final result:

$$\mathcal{Z} = \int Z_0^V d \langle \bar{\chi} \chi \rangle \tag{80}$$

where V is the three dimensional space volume and $Z_0 = Z_0(\langle \bar{\chi} \chi \rangle, T, \mu)$ is the effective partition function for $\langle \bar{\chi} \chi \rangle$. A standard saddle point analysis gives the condensate as a function of temperature and density, and allows for the reconstruction of the phase diagram.

The results are the following : below a critical temperature, there is a chiral transition as a function of chemical potential, closely correlated with a deconfining transition, from a normal phase to a ‘quark–gluon plasma’ phase. This transition is first order, very strong at zero temperature, and weakens with temperature, becoming second order at $\mu = 0, T = T_c$. The phase diagram is qualitatively similar to that of the Gross Neveu model, but for the fact that here we have also deconfinement correlated with the chiral transition.

8.2 The Phase Diagram of Two Color QCD

At the beginning of this section it is useful to remind ourselves of the discussion in Section 7.2: in a nutshell, $SU(2)$ baryons are completely degenerate with mesons, hence there are massless baryons. Both on physical grounds, and from the predictions of simple models (Gros–Neveu, Section 5) we know that the scale of critical phenomena at finite density is set

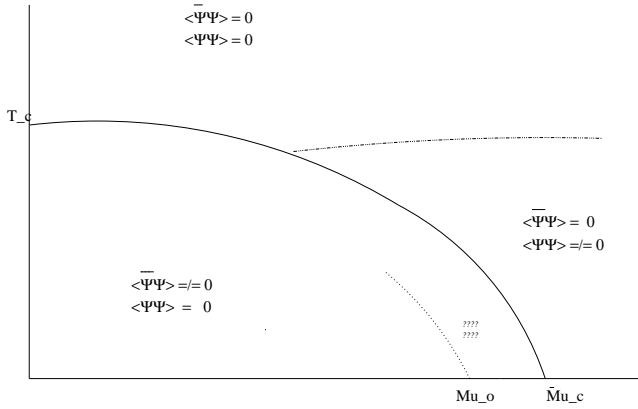


Figure 10: A sketchy view of the phase diagram of two colors QCD for a non-zero quark mass

by the lighter particle carrying baryon number—the massless diquark in two color QCD, and the massive baryon in QCD. Hence, two colors QCD is not a good approximation to real QCD at finite density.

Still, one might hope to learn something there, in particular concerning the gauge field dynamics and screening properties at nonzero baryon density [47]. In Fig. 10 I sketch a possible (i.e. suggested by the results of refs. [47]) phase diagram of two color QCD, in the chemical potential–temperature plane, for an arbitrary, non-zero bare quark mass. The general features of the theory at zero density, i.e. the $\mu = 0$ axis has been discussed in Sections 7.2 and 7.4 above.

When $\mu \neq 0$ quarks and antiquarks do not belong any more to equivalent representations: the Pauli–Gürsey symmetry is broken by a finite density. When $\mu \neq 0$ the symmetry is reduced to that of ‘normal’ QCD— just because the extra symmetry quark-antiquark is explicitly broken: the condensate will tend to rotate in chiral space as μ increases, rotating into a purely diquark direction for large μ . However, as μ increases and the symmetry in chiral space is reduced, and the new vacuum would be physically distinct from the original one. According to the standard scenario, at zero temperature, for a chemical potential μ_o comparable with the mass of the lightest baryons, baryons start to be produced thus originating a phase of cold, dense matter. For $SU(2)$ baryons (diquarks) are bosons (as opposed to the fermionic baryons of real QCD). Besides the mass scale of the phenomenon, there are then other important differences between the dense phase in $SU(2)$ and $SU(3)$, as, obviously, the thermodynamics of interacting Bose and Fermi gases is different. In particular, diquarks might well condense, however partial quark liberation is possible as well. We might then expect a rather complicated “mixed” nuclear matter phase, perhaps characterised by both types of condensates – this is the region marked by question marks in Figure 10.

To obtain a more direct probe of deconfinement, we can look at the interquark potential by calculating the correlations $\langle P(O)P^\dagger(z) \rangle$ of the zero momentum Polyakov loops, averaged over spatial directions. This quantity is related to the string tension σ via $\langle P(O)P^\dagger(z) \rangle \propto e^{-\sigma z}$. Some of the results of [47] suggests indeed fermion screening, enhanced string breaking and the transition to a deconfined phase. Gauge field dynamics can also be probed by measurements of the topological charge, as well as by the direct analysis of the Dirac spectrum [47].

8.3 The Phase Diagram of QCD

We reproduce in Figure 11 the phase diagram of QCD from Ref. [48].

Let us discuss the case of two massless flavors first. The transition with $\mu = 0$ has been discussed at length in Section 7.5 above : it should be second order, in the universality class of the $O(4)$ model. The study of the high baryon density transition at $T = 0$ meets with the problems discussed before in this Section. Nevertheless, the model calculations of [13], the lattice numerical results for the Gross- Neveu model reviewed in Section 5, the lattice strong coupling results discussed above suggests a strong first order transition. If this is the case, a tricritical point should be found where the first order line and the second order one merges along the phase diagram. This is the point P.

What happens if we consider light (rather than massless) up and down quarks, while still keeping the strange very large? The possibility considered in [48] is that the second order line turns into a smooth crossover, while the first order line is robust with respect to this perturbation. The tricritical point now becomes the end point E of the first order transition line. The effects of a not-so-heavy strange quark mass can be very important : remember that the transition for three massless flavors would be first order, hence for three light flavor should remain first order as well, and the point P would disappear. However this does not seem likely as the mass difference between up/down and strange is sizeable.

These aspects can be studied by considering the associate Ginzburg Landau effective potential for the order parameter $\langle \bar{\psi}\psi \rangle$, and the critical properties of the point E can again be inferred by universality arguments. The same model calculations have produced estimates for the position of the points P and E: $T_P \sim 100$ MeV and $\mu_P \sim 600 - 700$ MeV. Of course these are crude estimates as only chiral symmetry and not the full gauge dynamics was taken into account.

Most important is the observation that the critical behaviour at the point E can be observed in ongoing and future experiments at RHIC and LHC : indeed, E would be a genuine critical point, even with massive quarks, characterised by a diverging correlation length and fluctuations.

This is a very interesting situation where theoretical analysis inspired by universality arguments, lattice results at zero density, model calculations at zero temperature have lead to a coherent picture and new predictions amenable to an experimental verifications.

What next? Imaginary chemical potential calculations might perhaps be used to gain information around T_c and small density: this might help refining our knowledge of points P and E. Moreover, it might well be worthwhile to extend the lattice strong coupling expansion by 1. including further terms 2. performing a more refined analysis of the properties of the effective potential. In particular it would be possible to study the position of P, whose leading order estimate is at $\mu = 0$: the transition is always first order, with the only exception of the zero density, high temperature transition. It would be very interesting to see if the tricritical point would indeed move inside the phase diagram. One final remark on calculational schemes: in addition to the Lagrangean approach there is also the Hmiltonian one[46]. Time is not discretised in the Hamiltonian approach, and for several reasons this might seem more appropriate for dealing with a finite density. Moreoever, the remarkable progress made by the condensed matter community on the sign problem over the last few years might perhaps be helpful in this approach.

The scenario envisaged by [32] [33] might have an impact on the phenomenological issues

considered here. Infact, if there is indeed one critical line extending from the $m_q = 0$ axis to $m_q = \infty$ as sketched in Fig. 8, the fate of the chiral transitions with a finite quark mass should be reconsidered. For instance, the second order chiral transition with two massless quarks would flow into the weak first order transition of the pure Yang Mills model in the infinite mass limit. Hence, apparently a small quark mass would not wash out the second order phase transition. Once again, only ab initio lattice calculations can settle the issue.

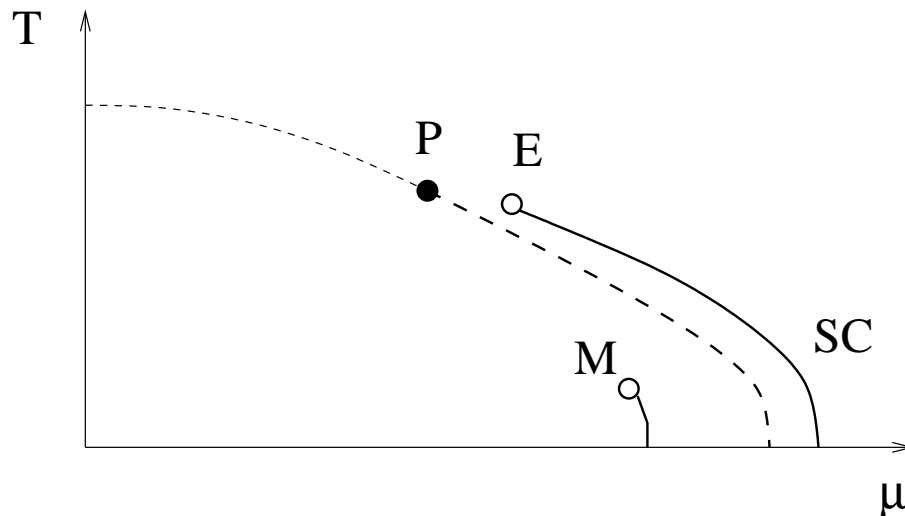


Figure 11: The schematic phase diagram of QCD, from ref. [48]. The dashed line is for the chiral transition for two flavor QCD, which is second order at $\mu = 0$ and most likely first order at $T=0$, hence a tricritical point P in between. The solid line is the relic of such phase transition with a small quark mass, and the tricritical point P turns into the endpoint E. The nuclear matter phase of QCD starts beyond the short line ending by M, which can be experimentally studied. The authors of [48] [49] have proposed experimental signatures to demonstrate the existence of, and locate the point E

Acknowledgments

I would like to thank the Organisers for a most enjoyable time in Trieste, as well as the Participants for many interesting conversations. In addition I thank the Institute for Nuclear Theory at the University of Washington and the U.S. Department of Energy for partial support. Part of the work described here was carried out at the Gran Sasso Laboratory in Italy, and while visiting the European Center for Theoretical Studies in Nuclear Physics and Related Areas, ECT*, Trento, Italy.

References

- [1] M. Quiros, *Finite Temperature Field Theory and Phase Transitions*, hep-ph/9901312;
- [2] V.A. Rubakov and M.E. Shaposhnikov, Phys.Usp.39 (1996)461, hep-ph/9603208;
- [3] J. Zinn-Justin, *Quantum Field Theory at Finite Temperature: an Introduction*, hep-ph/0005272;
- [4] D. Boyanovsky, *Phase Transitions in the Early and the Present Universe: from the Big Bang to Heavy Ion Collisions*, hep-ph/0102120 ;
- [5] M. Thoma, *New Developments and Applications of Thermal Field Theory*, hep-ph/0010164;
- [6] D. Bodeker, *Non Equilibrium Field Theory*, hep-lat/0011077;
- [7] M. Laine and K. Rummukainen, Nucl. Phys. Proc. Suppl.73 (1999) 180, hep-lat/9809045;
- [8] M. Laine, *Electroweak Phase Transition Beyond the Standard Model*, hep-ph/0010275 ;
- [9] K. Kajantie, M.Laine, K.Rummukainen, M.Shaposhnikov, Phys. Rev. Lett. 77 (1996) 2887 , hep-ph/9605228;
- [10] K. Kajantie, M. Laine, K. Rummukainen and M. Shaposhnikov, Nucl. Phys. B 493 (1997) 413, hep-lat/9612006
- [11] K. Kajantie, M. Laine, K. Rummukainen and M. Shaposhnikov, Nucl. Phys. B 458 (1996) 90;
- [12] J.-P. Blaizot and E. Iancu *The Quark Gluon Plasma: Collective Dynamics and Hard Thermal Loops*, hep-ph/0101103;
- [13] M. Alford, *Color Superconducting Quark Matter*, hep-ph/0102047; K. Rajagopal and F. Wilczek, *The Condensed Matter Physics of QCD*, to appear in 'At the Frontier of Particle Physics / Handbook of QCD', M. Shifman, ed., (World Scientific), hep-ph/0011333; R. Rapp, T. Schafer, E.V. Shuryak, M. Velkovsky , Annals Phys.280 (2000)35, hep-ph/9904353;
- [14] J. M. Cline, Pramana 55 (2000) 33 hep-ph/0003029
- [15] Introductory material on the lattice approach to field theory can be found in J. B. Kogut, Rev.Mod.Phys.51 (1979) 659; M. Creutz, *Quarks, Gluons and Lattice*, Cambridge; C. Itzykson-Douffre, *Statistical Field Theory*, Cambridge, Chapter 7;
- [16] An introduction to numerical simulations of lattice QCD thermodynamics is C. DeTar, in Hwa, R.C. (ed.): Quark-gluon plasma, vol.2 , pag. 1, hep-ph/9504325 ;

- [17] B. Petersson *High temperature QCD and dimensional reduction*, talk given at *International Workshop on Non-Perturbative Methods and Lattice QCD*, Guangzhou, China, 15-21 May 2000, [hep-lat/0009016](#)
- [18] A. Kocić, J.B. Kogut and M.-P. Lombardo, Nucl.Phys.B398 (1993) 376, [hep-lat/9209010](#), and references therein;
- [19] L.A. Fernandez, J.J. Ruiz-Lorenzo, M.-P. Lombardo and A. Tarancon, Phys.Lett. B 277 (1992) 485;
- [20] R. D. Pisarski and F. Wilczek , Phys.Rev. D29 (1984)338 ;
- [21] J. Engels, S. Mashkevich, T. Scheideler, G. Zinovev , Phys.Lett.B365 (1996) 219, [hep-lat/9509091](#) ;
- [22] L. Dolan and R. Jackiw, Phys. Rev. D9 (1974) 3320;
- [23] M. Gleiser and E.W. Kolb, Phys. Rev D48 (1993) 1560, [hep-ph/9208231](#)
- [24] These points are covered in many textbooks, a concise introduction can be found in Vilenkin-Shellard, *Cosmic strings and other topological defects*, chap. 2;
- [25] There has been steady progress on chiral fermions, the field is evolving, several formulations are currently under scrutiny, and are already producing results, which will hopefully soon reach the same quantitative accuracy of standard calculations. I would like to thank S. Randjbar-Daemi for conversations on this subjects.
- [26] K.G. Klimenko, Z.Phys. C 37 (1988) 457; Phys.Part.Nucl. 29 (1998)523
- [27] B. Rosenstein, B. Warr, S.H. Park Phys.Rept.205 (1991) 59;
- [28] For a review on four fermion models thermodynamic see S. Hands , Nucl.Phys.A642 (1998) 228, [hep-lat/9806022](#); see also S. Hands, S. Kim, J. B. Kogut, Nucl.Phys.B442 (1995) 364; [hep-lat/9501037](#), F. Karsch, J. B. Kogut, Nucl.Phys.B280 (1987) 289;
- [29] J.B. Kogut, C.G. Strouthos, Phys.Rev.D63 (2001)054502,2001 [hep-lat/9904008](#); J.B. Kogut, M.A. Stephanov, C.G. Strouthos, Phys.Rev.D58 (1998) 096001, [hep-lat/9805023](#) ;
- [30] See Chapter 8 of the classic book J. Kapusta, *Finite Temperature Field Theory*, for an introduction to QCD thermodynamics and phase transition, as well as H. Meyer-Ortmanns , Rev.Mod.Phys.68 (1996) 473;
- [31] N. Cabibbo and G. Parisi, Phys.Lett.B59 (1975)67;
- [32] A. Di Giacomo, Nucl.Phys. A663 (2000)199, [hep-lat/9907029](#) , Nucl.Phys.A661 (1999) 13 [hep-lat/9907010](#);
- [33] H. Satz, Nucl.Phys.A681 (2001) 3, [hep-ph/0007209](#);

- [34] Lattice calculations of QCD phase transitions and properties of the high temperature phase are continuously improving, sharpening the current understanding described here, which stems from about twenty years of lattice activity in the field. The thermodynamic reviews at the yearly Lattice Conference provides a more technical and complete summary, together with a complete list of references, see for instance F. Karsch, Nucl.Phys.Proc.Suppl.83 (2000) 14, [hep-lat/9909006](#);
- [35] F. R. Brown et al. Phys.Rev.Lett.65 (1990)2491
- [36] Th. Appelquist, P.S. Rodrigues da Silva, F. Sannino , Phys.Rev.D60 (1999) 116007 , [hep-ph/9906555](#);
- [37] J.B. Kogut and D.K. Sinclair, Phys.Lett.B492 (2000) 228 [hep-lat/0005007](#);
- [38] E. Shuryak, Comments Nucl.Part.Phys.21 (1994) 235, [hep-ph/9310253](#); MILC Collaboration, C. Bernard et al. Phys.Rev.Lett.78 (1997) 598, [hep-lat/9611031](#);
- [39] J. Wirstam, Phys.Rev.D62 (2000) 045012, [hep-ph/9912446](#);
- [40] C. Korthals-Altes, A. Kovner, Phys.Rev.D62 (2000) 096008,[hep-ph/0004052](#) ; C. Korthals-Altes, A. Kovner, M. Stephanov, Phys.Lett.B469 (1999) 205, [hep-ph/9909516](#) ;
- [41] R. D. Pisarski, Phys.Rev.D62 (2000) 111501, [hep-ph/0006205](#);
- [42] M.-P. Lombardo, Nucl.Phys.Proc.Suppl.83 (2000) 375, [hep-lat/9908006](#) , and references therein; A. Hart, M. Laine, O. Philipsen, Phys. Lett. B, to appear, [hep-lat/0010008](#);
- [43] For a review of the current status and perspectives of lattice finite density, see O. Philipsen, Nucl.Phys.Proc.Suppl.94 (2001) 49. A very recent proposal is M. Alford, S. Chandrasekharan, J. Cox, U.J. Wiese, [hep-lat/0101012](#);
- [44] M. Campostrini, P. Rossi, E. Vicari , Phys.Rev.D51 (1995) 958, [hep-lat/9406014](#);
- [45] For strong coupling expansion and applications to QCD thermodynamics see e.g. P. Damgaard, Phys.Lett. B143 (1984) 210, van den Doel, Z.Phys. C29 (1985) 79, F. Ilgenfritz et al., Nucl.Phys. B377 (1992) 651, N. Bilic, D. Demeterfi and B. Petersson, Phys.Rev. D37 (1988) 3691; In the discussion of strongly coupled QCD I followed this last paper. The others give comparable results.
- [46] Recent works on QCD thermodynamics in the Hamiltonian formalism include X-Q Luo, E. B. Gregory, S.-H. Guo, H. Kroger , [hep-ph/0011120](#) ; E. B. Gregory, S.-H. Guo, H. Kroger, X.-Q. Luo Phys.Rev.D62 (2000) 054508, [hep-lat/9912054](#); Y. Umino [hep-ph/0012071](#), Phys.Lett.B492 (2000) 385 [hep-ph/0007356](#);
- [47] S. Hands, J. B. Kogut, M.-P. Lombardo, S. E. Morrison, Nucl.Phys.B558 (1999) 327, [hep-lat/9902034](#) , and references therein. Recent lattice works on the same model includes S. Muroya, A. Nakamura, C. Nonaka Nucl.Phys.Proc.Suppl.94 (2001) 469, [hep-lat/0010073](#) ; B. Alles, M. D'Elia, M.-P. Lombardo, Nucl.Phys.Proc.Suppl.94

- (2001) 441, [hep-lat/0010068](#); S.J. Hands, J. B. Kogut, S.E. Morrison, D.K. Sinclair, Nucl.Phys.Proc.Suppl.94 (2001) 457, [hep-lat/0010028](#) ; E. Bittner, M.-P. Lombardo, H. Markum, R. Pullirsch , Nucl.Phys.Proc.Suppl.94 (2001) 445, [hep-lat/0010018](#) ; R. Aloisio, V. Azcoiti, G. Di Carlo, A. Galante, A.F. Grillo, Phys.Lett.B493:189-196,2000, [hep-lat/0009034](#) S. Hands, I. Montvay, S. Morrison, M. Oevers, L. Scorzato, J. Skullerud; Eur.Phys.J.C17 (2000) 285 [hep-lat/0006018](#) ; M.-P. Lombardo [hep-lat/9907025](#) ;
- [48] M. Stephanov, K. Rajagopal, E. Shuryak, Phys. Rev. Lett Phys.Rev.Lett.81 (1998) 4816; J. Berges and K. Rajagopal, Nucl.Phys. B538 (1999) 215, [hep-ph/9804233](#); M.A. Halasz, A.D. Jackson, R.E. Shrock, M.A. Stephanov and J.J.M. Verbaarschot, Phys.Rev.D58 (1998) 096007, [hep-ph/9804290](#);
- [49] E.V. Shuryak and M.A. Stephanov , [hep-ph/0010100](#); M. Stephanov, K. Rajagopal, E. Shuryak, Phys.Rev.D60 (1999) 114028, [hep-ph/9903292](#).